

Self-Assembly of Lanthanide-Covalent Organic Polyhedra: Chameleonic Luminescence and Efficient Catalysis

Shi-Long Han,^{||} Jian Yang,^{||} Debakanta Tripathy, Xiao-Qing Guo, Shao-Jun Hu, Xiao-Zhen Li, Li-Xuan Cai, Li-Peng Zhou, and Qing-Fu Sun*

Cite This: <https://dx.doi.org/10.1021/acs.inorgchem.0c01780>

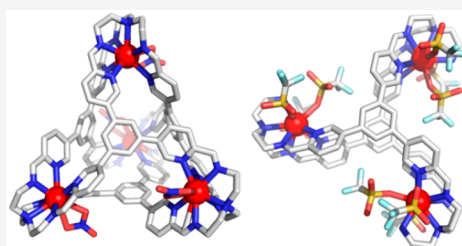
Read Online

ACCESS |

Metrics & More

Article Recommendations

Supporting Information



- ✓ Lanthanide-covalent organic polyhedra
- ✓ Chameleonic luminescence
- ✓ Efficient catalysis

ABSTRACT: A series of multinuclear lanthanide-covalent organic polyhedra (LnCOPs), including pillar-typed triangular prisms **1-Ln₃** and tetrahedra **2-Ln₄** (Ln = La^{III}, Sm^{III}, Eu^{III}), have been constructed for the first time, through either one-pot subcomponent self-assembly or postassembly metalation. In contrast to the known tetrahedral cages based on transition metals, the pillar-typed polyhedra were favored from the same organic components in the presence of lanthanides. Besides this, facile transmetalations between the **1-Ln₃** polyhedra endow cascade chameleonic luminescence. Meanwhile, the open metal sites and pendent amine groups on **1-Ln₃** enable these polyhedra to catalyze the Henry reaction efficiently.

INTRODUCTION

Molecular polyhedra are attractive compounds because of their appealing structures and potential applications in separation, catalysis, recognition, etc.¹ Discrete metallosupramolecular polyhedra formed through the coordination-directed assembly approach have witnessed fast development in the past decades because of the well-established synthetic strategy as well as their fascinating functions.² Meanwhile, porous covalent polyhedra constructed through dynamic covalent chemistry have gained increasing attention recently, due to their high stability, good solubility, and facile functionalization.³ Up to now, the function of covalent organic polyhedra has depended largely on the organic ligands and their defined cavity.⁴ It is natural to expect that metal decoration onto the covalent organic polyhedra will bring diversified properties and functions.

With regard to their intrinsic optical, electromagnetic, and catalytic properties,⁵ we envisage that introduction of the lanthanides with supramolecular architectures will create a new class of functional compounds.⁶ Previously, subcomponent self-assembly of ligand **L** possessing three pyridyl aldehyde groups, tris(2-aminoethyl)amine (TREN), and transition metals (M = Zn, Fe, Cd) was reported to give tetrahedral polyhedra.⁷ With seven coordination sites available at each vertex (four N atoms from TREN and three N atoms from pyridyls) on this polyhedron, this skeleton is ideal for construction of lanthanide-covalent organic polyhedra

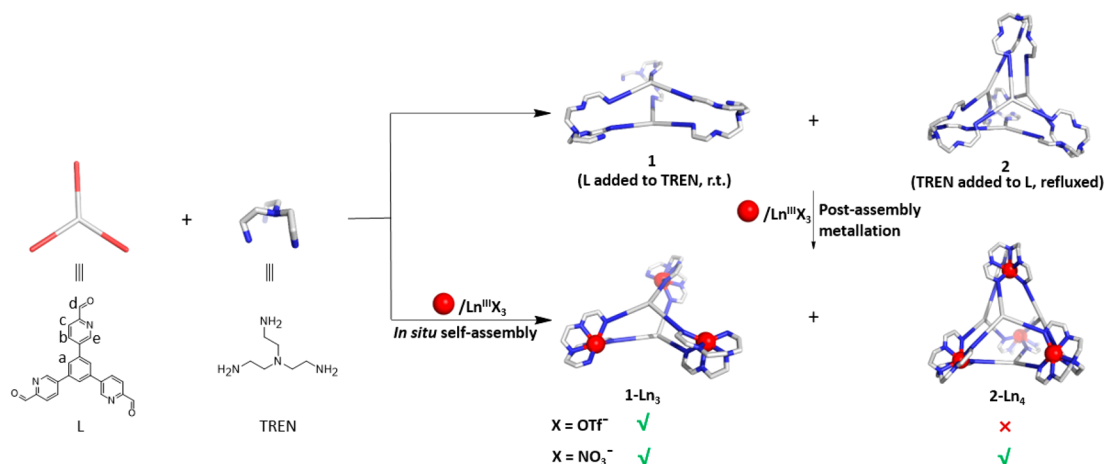
(LnCOPs), which will combine both a supramolecular cavity and unsaturated coordinated metal sites on one single polyhedron.

Herein, we report for the first time the syntheses of a series of such multinuclear LnCOPs. In contrast to the known tetrahedral polyhedra formed with transition-metals, the combination of **L**, TREN, and trivalent lanthanide ions (Ln^{III}) favors the formation of **1-Ln₃** pillared polyhedra, either through one-pot subcomponent self-assembly or postassembly metalation (Scheme 1). Transmetalation transformations were realized from **1-La₃** to other isostructural **1-Ln₃** (Ln = Sm^{III}, Eu^{III}) polyhedra, resulting in chameleonic changes in emission color. Taking advantage of the available open metal sites and pendent amine groups on the LnCOPs, we also demonstrated that they are able to catalyze the Henry reaction in high yield.

RESULTS AND DISCUSSION

Our first idea was to start with the preparation of an empty [4 + 4] organic polyhedron **2** from **L** and TREN and then do postassembly metalation to obtain the **2-Ln₄** complexes.

Received: June 16, 2020

Scheme 1. Two Synthetic Routes toward the Self-Assembly of 1-Ln₃ and 2-Ln₄

However, it turned out to be not straightforward; direct reaction of equimolar L with TREN in one portion at 2.5 mM concentration gave a mixture of **1** and **2** (Figures S29 and S30). Interestingly, dropwise addition of TREN into a highly dilute solution of L in chloroform (0.25 mM) at refluxed temperature led to pure polyhedron **2** quantitatively (Figures 1D and S7–S11), while inverse addition (L added into TREN)

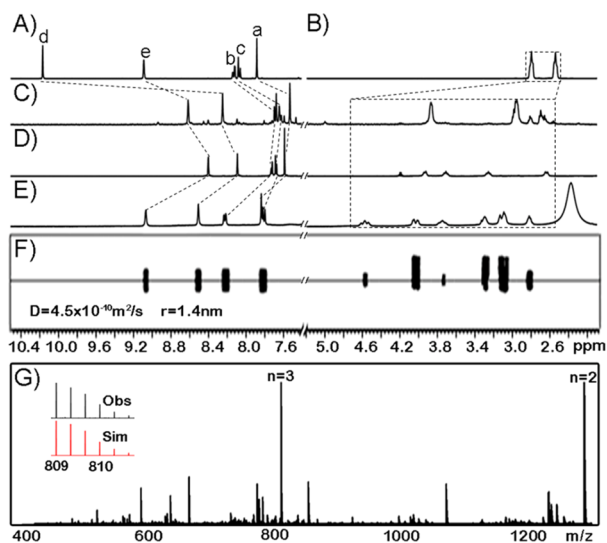


Figure 1. Partial ¹H NMR spectra (A–D, 400 MHz, CDCl₃, 298 K) of (A) L, (B) TREN, (C) **1**, (D) **2**, and (E) **1-La₃** (600 MHz, CD₃CN, 298 K); (F) ¹H DOSY spectra of **1-La₃**; and (G) ESI-TOF-MS spectrum of **1-La₃·(OTf)₉**. Signals in the dashed square are from TREN.

at room temperature gave an exclusive formation of [2 + 3] polyhedron **1** (Figures 1C and S2–S6), indicating that the addition order determined the formation of either **1** or **2**.^{3e} To be mentioned, **1** and **2** were observed to interconvert to each other gradually in solution because of the nature of dynamic covalent imine bond (Figures S31 and S32).

We envisaged that, upon metallation, the tetrahedral conformation of polyhedron **2** could be fixed. Unexpectedly, addition of Ln(OTf)₃ to the solution of freshly prepared polyhedron **2** led to the formation of **1-Ln₃**, exclusively. The downfield shifting of protons was observed for the ¹H NMR spectrum, indicating the complexation with La^{III} ions (Figure

1E). Diffusion-ordered NMR spectroscopy (DOSY) shows that all signals have the same diffusion coefficient, confirming the formation of a single species (Figure 1F). Electrospray ionization time-of-flight mass spectroscopy (ESI-TOF-MS) indicated the formation of a complex with a formula of **1-La₃·(OTf)₉**, instead of a tetrahedral **2-La₄·(OTf)₁₂** (Figure 1G). It was speculated that the Lewis acidity of lanthanides acted as catalysts to accelerate the conversion of **2** to **1** during this process, and the coordination requirements of lanthanides could drive this process as well.

One-pot subcomponent self-assembly gave similar results. Reaction of equimolar L, TREN, and La(OTf)₃ in CD₃CN at 50 °C for 5 h led to a homogeneous yellow solution whose spectroscopic data were consistent with those for **1-Ln₃** observed above. Transmetalation from the known **2-Zn₄** tetrahedral polyhedron to **2-La₄** was not successful (Figure S37), possibly due to the weaker coordination nature of lanthanides compared to transition metals. Other isostructural **1-Ln₃** type (Ln = Sm, Eu) LnCOPs could also be synthesized in a similar manner by replacing La(OTf)₃ with the corresponding metal sources, whose formation were also confirmed by ¹H, COSY, and DOSY NMR and ESI-TOF-MS (Figures S17–S23).

Suitable crystals of **1-Eu₃** were obtained by slow vapor diffusion of diethyl ether into an acetonitrile solution of the complex. X-ray diffraction analysis shows that this trinucleate complex crystallized in the P6(3)/m space group. As shown in Figure 2A and 2C, each Eu^{III} center is nine-coordinated with two pyridyl N atoms, four N atoms of the TREN unit, and three O atoms of three OTf⁻; the Eu^{III} centers are separated by 11.7 Å. Unexpectedly, one of the –NH₂ amino group on the TREN was unreacted, probably due to larger ionic radii and irregular coordination geometries for lanthanides compared to transition metals.

Counterions are known to influence the assembly process and have crucial impact on the structural formation.⁸ Subcomponent self-assembly of equimolar L, TREN, and Ln(NO₃)₃·6H₂O (Ln = La^{III}, Sm^{III}, Eu^{III}) instead of using Ln(OTf)₃ in CD₃CN resulted in insoluble suspension. Because of bad solubility, NMR spectra could not give any useful information. However, ESI-TOF-MS for the filtrate suggested the formation of a mixture of **1-Ln₃** and **2-Ln₄** (Figures S24–S26), neither of which could be isolated. This is clearly different from the exclusive formation of **1-Ln₃**, when

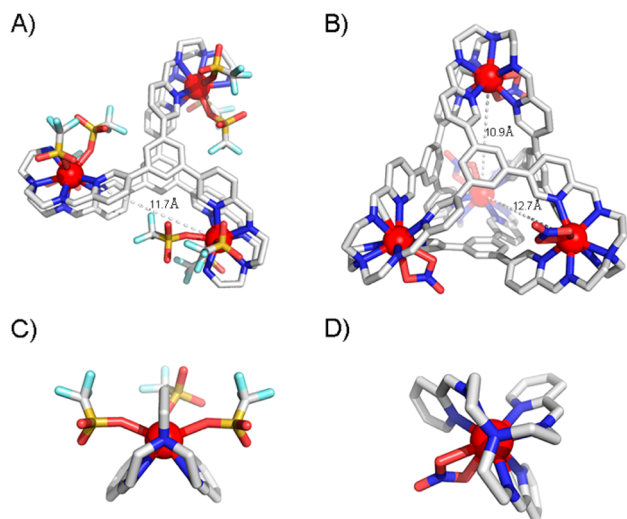


Figure 2. X-ray crystal structures of (A) $1\text{-Eu}_3\cdot(\text{OTf})_9$ and (B) $2\text{-Eu}_4\cdot(\text{NO}_3)_{12}$. Eu–Eu distances are indicated by dashed lines. (C) The coordination geometries on the Eu centers of $1\text{-Eu}_3\cdot(\text{OTf})_9$. (D) The coordination geometries on the Eu centers of $2\text{-Eu}_4\cdot(\text{NO}_3)_{12}$. Hydrogen and the counterion are omitted for clarity. Color code: red, Eu; gray, C; reddish, O; blue, N; yellow, S; cyan, F.

$\text{Ln}(\text{OTf})_3$ salts were used. The formation of the 2-Eu_4 was also unambiguously established from an exiguous crystal obtained by slow evaporation of the acetonitrile mixture. X-ray diffraction analysis shows that this tetranucleate complex crystallized in the $Pca2(1)$ space group. As anticipated, the 2-Eu_4 polyhedron displays a distorted tetrahedral conformation where four Eu^{III} ions sit on the vertices and four ligands span the faces (Figure 2B). Due to the large ionic radius and higher coordination numbers of the Eu^{III} ions, each metal center is nine-coordinated with three pyridyl N atoms, four N atoms of TREN, and two O atoms of one NO_3^- anion (Figure 2D). The coordination of NO_3^- ions on the vertices reduces the T symmetry of the polyhedron into a C_2 symmetry, which is quite different from that of the previously reported 2-Zn_4 polyhedron. As a result, the six edges (defined by the Eu–Eu distances) of the tetrahedron are unequal, with four edges measured to be 12.2–12.7 Å and the remaining two orthogonally arranged edges being 10.9 Å.

Based on our previous finding on that the formation constants for different lanthanide-organic tetrahedra of the same ligand show exponential growth across the light-to-heavy lanthanide series,⁹ a transmetalation transformation starting from polyhedron 1-La_3 to other polyhedra 1-Ln_3 ($\text{Ln} = \text{Sm}, \text{Eu}$) was then tested. Indeed, when $\text{Sm}(\text{OTf})_3$ (1 equiv) was added to 1-La_3 (1 equiv), compared to metal ions prepared from one-pot synthesis, ^1H NMR indicated the instant metal-ion metathesis with the quantitative formation of the 1-Sm_3 (Figure S33). Similar transformation for $1\text{-La}_3 \rightarrow 1\text{-Eu}_3$ was also achieved (Figure S35).¹⁰ However, transmetalation between the neighboring lanthanides, i.e., $1\text{-Sm}_3 \rightarrow 1\text{-Eu}_3$, requires the addition of a large excess amount of Eu^{III} salts (Figure S34). It is worth noting that a cascade transformation of $1\text{-La}_3 \rightarrow 1\text{-Sm}_3 \rightarrow 1\text{-Eu}_3$ was also successful (Figure S36). Such metal-ion triggered transformations between different LnCOPs have also been confirmed by the luminescence titration experiments (see discussion below).

Photophysical studies confirmed that the organic polyhedron can sensitize the lanthanide luminescence in the visible

region. The excitation and luminescence spectra of 1-Ln_3 ($\text{Ln} = \text{Sm}^{\text{III}}, \text{Eu}^{\text{III}}$) polyhedra are displayed in Figure 3. Upon

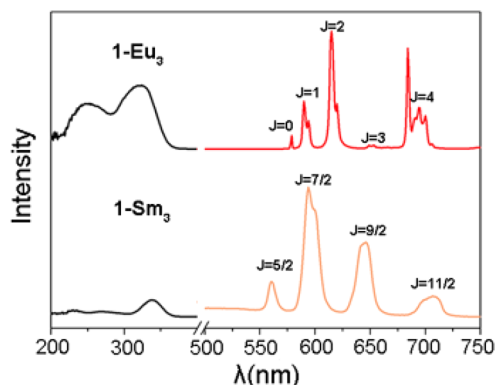


Figure 3. Excitation (black-dashed lines) and emission (solid color lines, for the visible region only) spectra of 1-Eu_3 and 1-Sm_3 in CH_3CN .

excitation at 324 nm in the ligand level, 1-Eu_3 displays characteristic line-like emission peaks at 580, 595, 615, 650, and 680 nm, corresponding to $^5\text{D}_0 \rightarrow ^7\text{F}_j$ ($J = 0\text{--}4$) transitions of Eu^{III} (Figure 3). The photoluminescent quantum yield (PLQY) of 1-Eu_3 is 5.07% in acetonitrile solution (Figure S56). Characteristic Sm^{III} emissions at 560, 595, 640, and 700 nm (corresponding to $^4\text{G}_{5/2} \rightarrow ^6\text{H}_j$, $J = 5/2\text{--}11/2$) were also obtained for 1-Sm_3 , but the sensitization efficiency was too low to be determined (Figure 3 and Figure S53). Besides this, metal-ion triggered chameleonic color changes were revealed by taking advantage of the fast and efficient transmetalation process. As shown in Figure 4A, with the addition of $\text{Sm}(\text{OTf})_3$ to 1-La_3 solution, the typical blue fluorescence at 450 nm arising from the ligand gradually weakened, accompanied by the evolving of the characteristic Sm^{III} emission.

When the quantity of Sm^{III} ions approaches 1 equiv, the intensity of Sm^{III} emission gets saturated, indicating complete conversion from 1-La_3 to 1-Sm_3 . Further addition of $\text{Eu}(\text{OTf})_3$ into the system led to a yellow-to-red color switching. The Eu^{III} emission kept getting stronger until 10 equiv of $\text{Eu}(\text{OTf})_3$ was added to the solution (Figure 4B). This is consistent with the ^1H NMR titration experiment (Figure S34). Proof-of-concept anticounterfeiting application was then demonstrated with the chameleonic property of these complexes. When **1** or 1-La_3 was used as the fluorescent ink, the blue printing pattern of **1** can be visualized under UV lamp (254 nm). When the pattern was smeared with the solution of $\text{Eu}(\text{OTf})_3$, the color changed into red immediately (Figure S49). As a control, no such blue-to-red color change could be observed when the ligand **L** was used (Figure S49), suggesting that construction of the organic polyhedron **1** is necessary for fast and stable chelation of the lanthanide ions.

Henry/Nitroaldol reaction is an important C–C bond formation reaction of nitroalkane with carbonyl compounds.¹¹ Shibaski et al. developed a series of rare-earth–binol complexes containing alkoxides as the base and rare-earth elements as Lewis acids for the efficient catalysis of Henry reactions.¹² 1-Ln_3 polyhedra with open metal sites and pendent amine groups provide ideal Lewis acid/base pairs for catalysis. We choose $\text{C}_6\text{H}_5\text{CHO}$, $p\text{-OHC}_6\text{H}_4\text{CHO}$, $p\text{-NO}_2\text{C}_6\text{H}_4\text{CHO}$, and nitromethane/nitroethane as typical substrates. When poly-

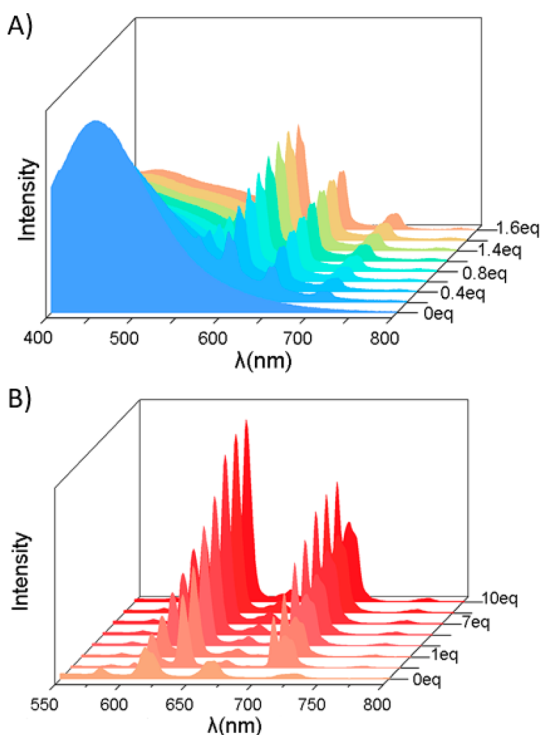
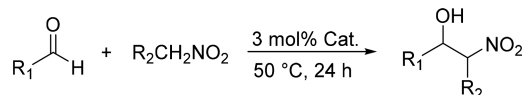


Figure 4. (A) Emission spectra of **1-La₃** (2.5×10^{-5} M in CH_3CN) with the addition of 0–1.6 equiv of $\text{Sm}(\text{OTf})_3$. (B) Emission spectra of **1-Sm₃** (2.5×10^{-5} M in CH_3CN) with the addition of 0–10 equiv of $\text{Eu}(\text{OTf})_3$.

hedron **1-La₃·(OTf)₉** (3 mol %) was used as the catalyst, a yield of 96% was reached after 24 h for $p\text{-NO}_2\text{C}_6\text{H}_4\text{CHO}$ (Table 1, entry 1). As a control, no product was obtained in

Table 1. Henry Reaction Catalyzed by LnCOPs^a



entry	catalyst	R ₁	R ₂	yield ^b (%)
1	1-La₃·(OTf)₉	$p\text{-NO}_2\text{C}_6\text{H}_4$	H	96
2	$\text{La}(\text{OTf})_3$	$p\text{-NO}_2\text{C}_6\text{H}_4$	H	0
3	1	$p\text{-NO}_2\text{C}_6\text{H}_4$	H	14 ^c
4	TREN	$p\text{-NO}_2\text{C}_6\text{H}_4$	H	34 ^c
5	2-Zn₄·(OTf)₈	$p\text{-NO}_2\text{C}_6\text{H}_4$	H	0
6	1-La₃·(OTf)₉	C_6H_5	H	8
7	1-La₃·(OTf)₉	$p\text{-OHC}_6\text{H}_4$	H	7
8	1-La₃·(OTf)₉	$p\text{-NO}_2\text{C}_6\text{H}_4$	CH_3	99
9	1-Sm₃·(OTf)₉	$p\text{-NO}_2\text{C}_6\text{H}_4$	H	29
10	1-Eu₃·(OTf)₉	$p\text{-NO}_2\text{C}_6\text{H}_4$	H	31
11	PAT-La	$p\text{-NO}_2\text{C}_6\text{H}_4$	H	92

^aReaction conditions: 5 mg of aldehyde, 0.5 mL of nitroalkane, 3 mol % catalyst at 50 °C for 24 h. ^bNMR yield based on aldehydes. ^cAlkene side product was observed.

the presence of $\text{La}(\text{OTf})_3$ (Table 1, entry 2). Though empty organic polyhedron **1** or TREN could also catalyze the reaction, only 14% and 34% yields were obtained, respectively, due to the formation of the eliminated alkene product (Table 1, entries 3 and 4), suggesting that the **1-La₃** was more efficient and selective. It is worth pointing out that the known **2-Zn₄** polyhedron could not catalyze this reaction, possibly due to its

saturated coordination on the metal centers (Table 1, entry 5). Besides, unsubstituted benzaldehyde and substrate with an electron-donating hydroxyl group failed to be activated under standard conditions (Table 1, entries 6 and 7). Less reactive nitroethane also gave a satisfactory result (Table 1, entry 8). Furthermore, both **1-Sm₃** and **1-Eu₃** showed low activity with much lower yields possibly due to its smaller ion radius compared with La^{III} , indicating that the nature of the lanthanide ions also plays an important role (Table 1, entries 1, 9, and 10, respectively). In order to verify the necessity of the framework of catalyst **1-La₃**, we mixed a 3:1:1 ratio of 2-picolinaldehyde, TREN, and $\text{La}(\text{OTf})_3$ to produce a noncage catalyst system **PAT-La**, which gave a similar yield (92%) compared to **1-La₃** under the same conditions (Table 1, entries 1 and 11). It seemed that the cage framework of the catalyst **1-La₃** does not have an obvious impact on the catalytic activity, possibly due to its barely available cavity (Figure 2A). Further exploration on the catalytic properties by virtue of the central cavity on such Ln-COPs complex is still underway.

Luminescent titrations were conducted to shed light on the reaction mechanism. With the addition of CH_3NO_2 to the solution of **1-Eu₃** in acetonitrile, the Eu^{III} emission was slightly enhanced, suggesting that nitromethane can compete with the coordinating solvent molecules that usually deactivate the luminescence of Eu^{III} . Moreover, addition of $p\text{-NO}_2\text{C}_6\text{H}_4\text{CHO}$ into **1-Eu₃** led to a significant decrease of the **1-Eu₃** emission, with a quenching constant K_{sv} of $1.026 \times 10^4 \text{ M}^{-1}$ calculated from the Stern–Volmer equation, indicating a strong interaction between substrate and catalyst (Figures S60 and S61).

CONCLUSIONS

In summary, we have shown that lanthanide functionalization on covalent organic polyhedra is feasible by both one-pot subcomponent self-assembly or postassembly metalation. The LnCOPs obtained in this study show interesting chameleonic emission properties and excellent catalytic performance. This work offers a new platform for the design of functional metal-containing covalent organic materials.

EXPERIMENTAL SECTION

General Information. All chemicals were purchased from commercial sources and used without further purification unless otherwise noted. Nuclear magnetic resonance (NMR) spectra were recorded using Bruker AVANCE III 400 or 600 MHz spectrometers. Chemical shifts are reported in ppm relative to the residual internal nondeuterated solvent signals. Electrospray ionization time-of-flight mass spectroscopy (ESI-TOF-MS) spectra were recorded on an Impact II UHR-TOF mass spectrometer from Bruker. Data analysis was conducted with the Bruker Data Analysis software (ver. 4.3), and simulations were performed with the Bruker Isotope Pattern software. UV–vis spectra are recorded on a UV-2700 UV–visible spectrophotometer from Shimadzu. Excitation and emission spectra were recorded on a F55 spectrophotometer from Edinburg Photonics.

Synthesis of L (1,3,5-Tris(4',4'',4'''-formylpyridine)-benzene). Ligand L was synthesized following a reported procedure.^{7a} Under a nitrogen atmosphere, to a solution of 1,3,5-tris(4,4,5,5-tetramethyl-1,3,2-dioxaborolan-2-yl)benzene (680 mg, 1.5 mmol) in dry DMF (120 mL) was added 5-bromo-2-pyridinecarboxaldehyde (1.25 g, 6.7 mmol), K_2CO_3 (3 g, 22 mmol), and $\text{Pd}(\text{PPh}_3)_4$ (516.9 mg, 0.44 mmol). The reaction mixture was stirred at 90 °C for 24 h. The solvent was removed under reduced pressure and the solid residue was triturated with water, collected by filtration, and washed with water (3 × 100 mL), hot diethyl ether (2 × 50 mL), and hot hexane (2 × 50 mL). The dried solid was triturated with CH_2Cl_2 and

collected again. The resulting solid was redissolved in hot CHCl_3 , and then the insoluble materials were filtered off and Et_2O was added to the filtrate to precipitate out pure product **L** as a pale solid (130 mg, 24%). ^1H NMR (400 MHz, CDCl_3 , 298 K): δ 10.18 (s, 3H), 9.12 (s, 3H), 8.19 (d, $J = 10.1$ Hz, 3H), 8.13 (d, $J = 8.1$ Hz, 3H), 7.95 (s, 3H). These data are consistent with those described in the literature.^{7a}

Synthesis of 1. To a solution of TREN (4.0 μL , 25 μmol , 1.5 equiv) in chloroform (20 mL) was added drop-wisely a solution of **L** (6 mg, 16 μmol , 1.0 equiv) in chloroform (5 mL). The reaction mixture was stirred at room temperature for half an hour. The reaction progress was monitored by ^1H NMR spectroscopy. After the reaction was completed, the reaction solution was washed with saturated aqueous K_2CO_3 three times. The organic phase was collected and dried over anhydrous Na_2SO_4 . Solvent was removed under reduced pressure to give **1** as a light yellow solid (6 mg, 67%). ^1H NMR (400 MHz, CDCl_3 , 298 K): δ 8.65 (s, 1H), 8.29 (s, 1H), 7.74 (d, $J = 8.2$ Hz, 1H), 7.69 (m, 1H), 7.58 (s, 1H), 3.84–3.75 (m, 2H), 2.97–2.85 (m, 3H), 2.81–2.70 (m, 1H), 2.68–2.61 (m, 1H). ^{13}C NMR (151 MHz, CDCl_3 , 298 K): δ 162.87, 153.63, 147.09, 138.63, 134.99, 134.10, 124.43, 120.67, 107.75, 90.16, 58.35, 52.76. ESI-TOF-MS for **1**: calcd $[\text{C}_{66}\text{H}_{72}\text{N}_{18} + \text{H}]^+$ 1117.6260, found 1117.6267; calcd $[\text{C}_{66}\text{H}_{72}\text{N}_{18} + 2\text{H}]^{2+}$ 559.3166, found 559.3163.

Synthesis of 2. To a solution of **L** (10 mg, 25 μmol , 1.0 equiv) in chloroform (100 mL) was added drop-wisely a solution of tris(2-aminoethyl)amine (TREN) (4.0 μL , 25 μmol , 1.0 equiv) in chloroform (5 mL). The reaction mixture was stirred and refluxed for 4 h. The reaction progress was monitored by ^1H NMR spectroscopy. After the reaction was completed, the reaction solution was washed with saturated aqueous K_2CO_3 three times. The organic phase was collected and dried over anhydrous Na_2SO_4 . Solvent was removed under reduced pressure to give **2** as a light yellow solid (8 mg, 66%). ^1H NMR (400 MHz, CDCl_3 , 298 K): δ 8.44 (s, 1H), 8.14 (s, 1H), 7.78 (dd, $J = 8.3, 2.1$ Hz, 1H), 7.73 (d, $J = 8.2$ Hz, 1H), 7.64 (s, 1H), 3.86 (d, $J = 9.8$ Hz, 1H), 3.65 (t, 1H), 3.20 (t, 1H), 2.59 (d, $J = 12.9$ Hz, 1H). ^{13}C NMR (151 MHz, CDCl_3 , 298 K): δ 162.14, 153.79, 147.11, 140.45, 136.34, 135.36, 126.13, 121.81, 59.20, 54.85. ESI-TOF-MS for **2**: calcd $[\text{C}_{120}\text{H}_{108}\text{N}_{28} + \text{Na}]^+$ 1964.9233, found 1964.9284.

General Procedure for Postassembly Metalation of 2 with $\text{Ln}(\text{OTf})_3$ and $\text{Ln}(\text{NO}_3)_3 \cdot 6\text{H}_2\text{O}$. To a suspension of **2** (5 mg, 1 equiv) in 600 μL of CD_3CN was added $\text{Ln}(\text{OTf})_3$ or $\text{Ln}(\text{NO}_3)_3 \cdot 6\text{H}_2\text{O}$ (4 equiv), and then the mixture was stirred at 50 $^\circ\text{C}$ for 1 h. The resulted mixture was filtered, and the filtrate was used for ^1H NMR and ESI-MS directly; the results showed no significant difference between one-pot subcomponent self-assembly (see below) and postassembly metalation in terms of the composition of the products. As demonstrated in the article text, this is probably because of the nature of a dynamic covalent imine bond and because Lewis acidity of lanthanides might accelerate the interconversion between **1** and **2**, and coordination modes of lanthanides prefer to form **1-Ln₃**-type structure due to efficient π - π stacking between two pillared ligand **L** in **1**. Consequently, **1-Ln₃** were obtained even though **2** was used. As a result, a one-pot subcomponent self-assembly strategy was used for constructing **1-Ln₃(NO₃)₉**, **1-Ln₃(OTf)₉**, and **2-Ln₄(NO₃)₁₂**, as described below for convenience.

Synthesis of 1-La₃(OTf)₉. To a suspension of **L** (5 mg, 12.7 μmol) and TREN (2.0 μL , 12.7 μmol) in 600 μL of CD_3CN was added $\text{La}(\text{OTf})_3$ (7.4 mg, 12.7 μmol), and then the mixture was stirred at 50 $^\circ\text{C}$ for 5 h. The turbid suspension gradually turned into a homogeneous pale brown solution. The solvent was removed under reduced pressure, and then the solid was washed with CHCl_3 (2×5 mL); pure product was obtained as a pale brown solid (yield 12 mg, 65%). ^1H NMR (400 MHz, CD_3CN , 298 K): δ 9.09 (s, 1H), 8.54 (s, 1H), 8.26 (d, $J = 9.4$ Hz, 1H), 7.88 (s, 1H), 7.85 (d, $J = 8.0$ Hz, 1H), 4.49 (t, $J = 15.3$ Hz, 1H), 4.01–3.92 (m, 1H), 3.74–3.62 (m, 1H), 3.23 (s, 1H), 3.06–2.98 (m, 2H), 2.80–2.74 (m, 1H). ^{13}C NMR (151 MHz, CD_3CN , 298 K): δ 167.07, 151.16, 147.80, 138.09, 137.78, 137.33, 127.61, 126.41, 58.19, 56.69, 49.21, 38.87, 36.76. ESI-TOF-MS for **1-La₃(OTf)₉**: calcd $[\text{1-La}_3(\text{OTf})_6]^{3+}$ 809.0161, found 809.0147.

Synthesis of 1-Sm₃(OTf)₉. To a suspension of **L** (5 mg, 12.7 μmol) and TREN (2.0 μL , 12.7 μmol) in 600 μL of CD_3CN was added $\text{Sm}(\text{OTf})_3$ (7.6 mg, 12.7 μmol), and then the mixture was stirred at 50 $^\circ\text{C}$ for 5 h. The turbid suspension gradually turned into a homogeneous pale brown solution. The solvent was removed under reduced pressure, and then the solid was washed with CHCl_3 (2×5 mL); pure product was obtained as a pale brown solid (yield 7 mg, 40%). ^1H NMR (600 MHz, CD_3CN , 298 K): δ 8.87 (s, 1H), 7.98 (d, $J = 7.6$ Hz, 1H), 7.88 (d, $J = 7.6$ Hz, 1H), 7.36 (s, 1H), 7.00 (s, 1H), 6.01 (s, 1H), 5.40 (s, 1H), 3.92 (d, $J = 16.1$ Hz, 1H), 2.17 (s, 1H), 1.85 (s, 1H), 1.50 (s, 2H). ^{13}C NMR (151 MHz, CD_3CN , 298 K): δ 171.53, 152.66, 146.87, 137.84, 136.46, 136.40, 127.53, 125.51, 58.15, 39.53, 37.17, 14.67. ESI-TOF-MS for **1-Sm₃(OTf)₉**: calcd $[\text{1-Sm}_3(\text{OTf})_6]^{3+}$ 821.0287, found 821.0293; calcd $[\text{1-Sm}_3(\text{OTf})_7]^{2+}$ 1306.0193, found 1306.0216.

Synthesis of 1-Eu₃(OTf)₉. To a suspension of **L** (5 mg, 12.7 μmol) and TREN (2.0 μL , 12.7 μmol) in 600 μL of CD_3CN was added $\text{Eu}(\text{OTf})_3$ (7.7 mg, 12.7 μmol), and then the mixture was stirred at 50 $^\circ\text{C}$ for 5 h. The turbid suspension gradually turned into a homogeneous pale brown solution. The solvent was removed under reduced pressure, and then the solid was washed with CHCl_3 (2×5 mL); pure product was obtained as a pale brown solid (yield 7 mg, 58%). Although the ^1H NMR spectrum was difficult to assign due to the paramagnetic nature of Eu^{III} . Mass spectrum and X-ray crystal structure analyses confirm the formation of **1-Eu₃(OTf)₉**, without doubt. ESI-TOF-MS for **1-Eu₃(OTf)₉**: calcd $[\text{1-Eu}_3(\text{OTf})_7]^{2+}$ 1308.0221, found 1308.0234.

General Procedure for One-Pot Subcomponent Self-Assembly of 1-Ln₃(NO₃)₉ and 2-Ln₄(NO₃)₁₂. To a suspension of **L** (5 mg, 12.7 μmol , 1 equiv) and TREN (2.0 μL , 12.7 μmol , 1 equiv) in 600 μL of CD_3CN was added $\text{Ln}(\text{NO}_3)_3 \cdot 6\text{H}_2\text{O}$ (12.7 μmol , 1 equiv), and then the mixture was stirred at 50 $^\circ\text{C}$ for 5 h. The resulted mixture was filtered, and the filtrate was used for ^1H NMR directly; however, no detectable signals were observed, probably because of the bad solubility of these nitrate-coordinated lanthanide complexes in acetonitrile. Other solvents like DMSO, DMF, and MeOH turned out to be not successful for dissolving these complexes either, even though these lanthanide assemblies were detected by ESI-TOF-MS to confirm the formation of **1-Ln₃(NO₃)₉** and **2-Ln₄(NO₃)₁₂** as a mixture in each reaction. ESI-TOF-MS for **1-La₃(NO₃)₉**: calcd $[\text{1-La}_3(\text{NO}_3)_5]^{4+}$ 635.0877, found 635.0877. ESI-TOF-MS for **2-La₄(NO₃)₁₂**: calcd $[\text{2-La}_4(\text{NO}_3)_8]^{4+}$ 748.3649, found 748.3641. ESI-TOF-MS for **2-Sm₄(NO₃)₁₂**: calcd $[\text{2-Sm}_4(\text{NO}_3)_9\text{-L}]^{2+}$ 920.8059 (note: under these MS conditions, one of the ligands was lost), found 920.8055. ESI-TOF-MS for **1-Sm₄(NO₃)₁₂**: calcd $[\text{1-Sm}_3(\text{NO}_3)_7]^{2+}$ 1001.6451, found 1001.6133. ESI-TOF-MS for **2-Eu₄(NO₃)₁₂**: calcd $[\text{2-Eu}_4(\text{NO}_3)_9\text{-L}]^{3+}$ 923.1420 (note: under these MS conditions, one of the ligands was lost), found 923.1411. ESI-TOF-MS for **1-Eu₃(NO₃)₉**: calcd $[\text{1-Eu}_3(\text{NO}_3)_6]^{3+}$ 648.4358, found 648.4356.

Synthesis of 2-Zn₄(OTf)₈. **2-Zn₄(OTf)₈** was synthesized according to the reported literature.^{7b} ESI-TOF-MS for **2-Zn₄(OTf)₈**: calcd $[\text{2-Zn}_4(\text{OTf})_3(\text{H}_2\text{O})]^{5+}$ 533.9015, found 533.9022; calcd $[\text{2-Zn}_4(\text{OTf})_5(\text{H}_2\text{O})]^{3+}$ 989.1375, found 989.1375; calcd $[\text{2-Zn}_4(\text{OTf})_6(\text{H}_2\text{O})]^{2+}$ 1558.1826, found 1558.1853. See ^1H NMR spectrum in the Supporting Information.

^1H NMR Titration for Transmetalation Transformations between 1-Ln₃(OTf)₉ (Ln = La^{III}, Sm^{III}, Eu^{III}) or between 2-Zn₄(OTf)₈ and 2-La₄(OTf)₁₂. To a solution of **1-La₃(OTf)₉** (1.0 mM in CD_3CN , 500 μL), an aliquot of a concentrated solution of $\text{Sm}(\text{OTf})_3$ (10 mM, CD_3CN) was titrated in NMR tube until transmetalation transformation completed as monitored by chemical shift. Transmetalation transformations between other **1-Ln₃(OTf)₉** were performed in the same way by replacement with corresponding lanthanide salts. Titration results showed that it was not successful for transmetalation transformation from **2-Zn₄(OTf)₈** to **2-La₄(OTf)₁₂**.

General Procedure for Catalytic Transformation of the Henry Reaction. To a reaction vial equipped with a stirring bar was added 5 mg of aldehyde, 0.5 mL of CH_3NO_2 or $\text{CH}_3\text{CH}_2\text{NO}_2$, and catalyst (3% mol), and the reaction mixture stirred at 50 $^\circ\text{C}$ for 24 h.

The solvent was evaporated under reduced pressure. The residue was dissolved in CDCl_3 (700 μL), and the yield was determined with 1,3,5-trimethoxybenzene (1 mg, 0.00595 mmol) as an internal standard.

Single-Crystal X-ray Diffraction Studies. Suitable single crystals for complexes **1-Eu₃-(OTf)₉** and **2-Eu₄-(NO₃)₁₂** were obtained by slowly evaporating their acetonitrile solution. The X-ray diffraction studies for **1-Eu₃-(OTf)₉** (CCDC code: 2002431) were carried out on a microfocus metaljet diffractometer using Ga $K\alpha$ radiation ($\lambda = 1.3405 \text{ \AA}$), and those for **2-Eu₄-(NO₃)₁₂** (CCDC code: 2002432) were carried out on a Bruker D8 VENTURE photon II diffractometer with an $I\mu\text{s}$ 3.0 microfocus X-ray source using the APEX III program. The structures were solved by direct methods and refined by full-matrix least-squares on F^2 with anisotropic displacement using the SHELX software package.¹³ The electron residuals in such cases were removed by the SQUEEZE routine.¹⁴

Crystal Data for 1-Eu₃-(OTf)₉. Space group $P63/m$; $a = b = 27.3224(10) \text{ \AA}$, $c = 17.4451(6) \text{ \AA}$; $\alpha = \beta = 90^\circ$, $\gamma = 120^\circ$; $V = 11278.2(9) \text{ \AA}^3$; $Z = 2$; $T = 299.09(11) \text{ K}$. Anisotropic least-squares refinement for the framework atoms and isotropic refinement for the other atoms on 4221 independent merged reflections [$R(\text{int}) = 0.1133$] converged at residual $wR_2 = 0.2848$ for all data; residual $R_1 = 0.0785$, $wR_2 = 0.2411$ [$I > 2\sigma(I)$], and goodness of fit (GOF) = 0.905.

Crystal Data for 2-Eu₄-(NO₃)₁₂. Space group $Pca2_1$; $a = 24.605(5) \text{ \AA}$, $b = 18.508(4) \text{ \AA}$, $c = 31.822(6) \text{ \AA}$; $\alpha = \beta = \gamma = 90^\circ$; $V = 14492(5) \text{ \AA}^3$; $Z = 4$; $T = 100 \text{ K}$. Anisotropic least-squares refinement for the framework atoms and isotropic refinement for the other atoms on 28413 independent merged reflections [$R(\text{int}) = 0.0867$] converged at residual $wR_2 = 0.2318$ for all data; residual $R_1 = 0.0801$, $wR_2 = 0.2022$ [$I > 2\sigma(I)$], and goodness of fit (GOF) = 1.032.

■ ASSOCIATED CONTENT

Supporting Information

The Supporting Information is available free of charge at <https://pubs.acs.org/doi/10.1021/acs.inorgchem.0c01780>.

Additional experimental details including figures and tables (PDF)

Accession Codes

CCDC 2002431–2002432 contain the supplementary crystallographic data for this paper. These data can be obtained free of charge via www.ccdc.cam.ac.uk/data_request/cif, or by emailing data_request@ccdc.cam.ac.uk, or by contacting The Cambridge Crystallographic Data Centre, 12 Union Road, Cambridge CB2 1EZ, UK; fax: +44 1223 336033.

■ AUTHOR INFORMATION

Corresponding Author

Qing-Fu Sun – College of Chemistry, Fuzhou University, Fuzhou 350108, People's Republic of China; State Key Laboratory of Structural Chemistry, Fujian Institute of Research on the Structure of Matter, Chinese Academy of Sciences, Fuzhou 350002, People's Republic of China; Fujian College, University of Chinese Academy of Sciences, Beijing 100049, People's Republic of China; orcid.org/0000-0002-6419-8904; Email: qfsun@fjirsm.ac.cn

Authors

Shi-Long Han – College of Chemistry, Fuzhou University, Fuzhou 350108, People's Republic of China; State Key Laboratory of Structural Chemistry, Fujian Institute of Research on the Structure of Matter, Chinese Academy of Sciences, Fuzhou 350002, People's Republic of China

Jian Yang – State Key Laboratory of Structural Chemistry, Fujian Institute of Research on the Structure of Matter, Chinese

Academy of Sciences, Fuzhou 350002, People's Republic of China

Debakanta Tripathy – State Key Laboratory of Structural Chemistry, Fujian Institute of Research on the Structure of Matter, Chinese Academy of Sciences, Fuzhou 350002, People's Republic of China

Xiao-Qing Guo – State Key Laboratory of Structural Chemistry, Fujian Institute of Research on the Structure of Matter, Chinese Academy of Sciences, Fuzhou 350002, People's Republic of China; Fujian College, University of Chinese Academy of Sciences, Beijing 100049, People's Republic of China

Shao-Jun Hu – State Key Laboratory of Structural Chemistry, Fujian Institute of Research on the Structure of Matter, Chinese Academy of Sciences, Fuzhou 350002, People's Republic of China; Fujian College, University of Chinese Academy of Sciences, Beijing 100049, People's Republic of China

Xiao-Zhen Li – State Key Laboratory of Structural Chemistry, Fujian Institute of Research on the Structure of Matter, Chinese Academy of Sciences, Fuzhou 350002, People's Republic of China

Li-Xuan Cai – State Key Laboratory of Structural Chemistry, Fujian Institute of Research on the Structure of Matter, Chinese Academy of Sciences, Fuzhou 350002, People's Republic of China

Li-Peng Zhou – State Key Laboratory of Structural Chemistry, Fujian Institute of Research on the Structure of Matter, Chinese Academy of Sciences, Fuzhou 350002, People's Republic of China; orcid.org/0000-0003-3820-2591

Complete contact information is available at:

<https://pubs.acs.org/doi/10.1021/acs.inorgchem.0c01780>

Author Contributions

^{||}These authors contributed equally.

Notes

The authors declare no competing financial interest.

■ ACKNOWLEDGMENTS

This work was supported by the National Natural Science Foundation of China (21825107, 21901245) and the Strategic Priority Research Program of the Chinese Academy of Sciences (XDB20000000).

■ REFERENCES

- (1) (a) Lehn, J. M. Cryptates: the chemistry of macropolycyclic inclusion complexes. *Acc. Chem. Res.* **1978**, *11*, 49–57. (b) Cram, D. J. The design of molecular hosts, guests, and their complexes (Nobel Lecture). *Angew. Chem., Int. Ed. Engl.* **1988**, *27*, 1009–1020. (c) Cram, D. J. Molecular container compounds. *Nature* **1992**, *356*, 29–36. (d) Conn, M. M.; Rebek, J. Self-assembling capsules. *Chem. Rev.* **1997**, *97*, 1647–1668. (e) Rebek, J., Jr. Molecular Recognition with Model Systems. *Angew. Chem., Int. Ed. Engl.* **1990**, *29*, 245–255.
- (2) (a) Fujita, M. Metal-directed self-assembly of two- and three-dimensional synthetic receptors. *Chem. Soc. Rev.* **1998**, *27*, 417–425. (b) Yoshizawa, M.; Klosterman, J. K.; Fujita, M. Functional Molecular Flasks: New Properties and Reactions within Discrete, Self-Assembled Hosts. *Angew. Chem., Int. Ed.* **2009**, *48*, 3418–3438. (c) Zhang, D.; Ronson, T. K.; Nitschke, J. R. Functional Capsules via Subcomponent Self-Assembly. *Acc. Chem. Res.* **2018**, *51*, 2423–2436. (d) Chakrabarty, R.; Mukherjee, P. S.; Stang, P. J. Supramolecular coordination: self-assembly of finite two- and three-dimensional ensembles. *Chem. Rev.* **2011**, *111*, 6810–6918. (e) Fiedler, D.; Leung, D. H.; Bergman, R. G.; Raymond, K. N. Selective molecular recognition, C-H bond activation, and catalysis in nanoscale reaction vessels. *Acc. Chem. Res.* **2005**, *38*, 349–358. (f) Wang, J.; He, C.; Wu, P.; Wang, J.; Duan, C.

An amide-containing metal–organic tetrahedron responding to a spin-trapping reaction in a fluorescent enhancement manner for biological imaging of NO in living cells. *J. Am. Chem. Soc.* **2011**, *133*, 12402–12405. (g) Howlader, P.; Zangrando, E.; Mukherjee, P. S. Self-assembly of enantiopure Pd12 tetrahedral homochiral nanocages with tetrazole linkers and chiral recognition. *J. Am. Chem. Soc.* **2020**, *142*, 9070–9078. (h) Lu, Y.; Zhang, H.-N.; Jin, G.-X. Molecular borromean rings based on half-sandwich organometallic rectangles. *Acc. Chem. Res.* **2018**, *51*, 2148–2158. (i) Han, M.; Engelhard, D. M.; Clever, G. H. Self-assembled coordination cages based on banana-shaped ligands. *Chem. Soc. Rev.* **2014**, *43*, 1848–1860. (j) Xiong, K.; Jiang, F.; Gai, Y.; Yuan, D.; Chen, L.; Wu, M.; Su, K.; Hong, M. Truncated octahedral coordination cage incorporating six tetranuclear-metal building blocks and twelve linear edges. *Chem. Sci.* **2012**, *3*, 2321–2325. (k) Fan, X.; Narayanam, N.; Gao, M.; Zhang, L.; Zhang, J. Ligand dependent assembly of trinuclear titanium-oxo units into coordination tetrahedra and capsules. *Dalton Trans.* **2018**, *47*, 663–665. (l) Liu, G.; Di Yuan, Y.; Wang, J.; Cheng, Y.; Peh, S. B.; Wang, Y.; Qian, Y.; Dong, J.; Yuan, D.; Zhao, D. Process-tracing study on the postassembly modification of highly stable zirconium metal–organic cages. *J. Am. Chem. Soc.* **2018**, *140*, 6231–6234.

(3) (a) Holst, J. R.; Trewin, A.; Cooper, A. I. Porous organic molecules. *Nat. Chem.* **2010**, *2*, 915–920. (b) Zhang, G.; Mastalerz, M. Organic cage compounds – from shape-persistency to function. *Chem. Soc. Rev.* **2014**, *43*, 1934–1947. (c) Rowan, S. J.; Cantrill, S. J.; Cousins, G. R. L.; Sanders, J. K. M.; Stoddart, J. F. Dynamic covalent chemistry. *Angew. Chem., Int. Ed.* **2002**, *41*, 898–952. (d) Zhang, D.; Martinez, A.; Dutasta, J.-P. Emergence of hemicryptophanes: from synthesis to applications for recognition, molecular machines, and supramolecular catalysis. *Chem. Rev.* **2017**, *117*, 4900–4942. (e) Jiao, T.; Wu, G.; Chen, L.; Wang, C.-Y.; Li, H. Precursor control over the self-assembly of organic cages via imine condensation. *J. Org. Chem.* **2018**, *83*, 12404–12410.

(4) (a) Jiao, T.; Chen, L.; Yang, D.; Li, X.; Wu, G.; Zeng, P.; Zhou, A.; Yin, Q.; Pan, Y.; Wu, B.; Hong, X.; Kong, X.; Lynch, V. M.; Sessler, J. L.; Li, H. Trapping white phosphorus within a purely organic molecular container produced by imine condensation. *Angew. Chem., Int. Ed.* **2017**, *56*, 14545–14550. (b) Qu, H.; Wang, Y.; Li, Z.; Wang, X.; Fang, H.; Tian, Z.; Cao, X. Molecular face-rotating cube with emergent chiral and fluorescence properties. *J. Am. Chem. Soc.* **2017**, *139*, 18142–18145. (c) Tromans, R. A.; Carter, T. S.; Chabanne, L.; Crump, M. P.; Li, H.; Matlock, J. V.; Orchard, M. G.; Davis, A. P. A biomimetic receptor for glucose. *Nat. Chem.* **2019**, *11*, 52–56. (d) Liu, Y.; Zhao, W.; Chen, C.-H.; Flood, A. H. Chloride capture using a C–H hydrogen-bonding cage. *Science* **2019**, *365*, 159–161.

(5) (a) Bünzli, J.-C. G.; Piguet, C. Taking advantage of luminescent lanthanide ions. *Chem. Soc. Rev.* **2005**, *34*, 1048–1077. (b) Bünzli, J.-C. G.; Piguet, C. Lanthanide-containing molecular and supramolecular polymeric functional assemblies. *Chem. Rev.* **2002**, *102*, 1897–1928. (c) Yan, B. Lanthanide-functionalized metal–organic framework hybrid systems to create multiple luminescent centers for chemical sensing. *Acc. Chem. Res.* **2017**, *50*, 2789–2798. (d) Guo, Y.-N.; Xu, G.-F.; Gamez, P.; Zhao, L.; Lin, S.-Y.; Deng, R.; Tang, J.; Zhang, H.-J. Two-step relaxation in a linear tetranuclear dysprosium(III) aggregate showing single-molecule magnet behavior. *J. Am. Chem. Soc.* **2010**, *132*, 8538–8539. (e) Mikami, K.; Terada, M.; Matsuzawa, H. Asymmetric catalysis by lanthanide complexes. *Angew. Chem., Int. Ed.* **2002**, *41*, 3554–3572. (f) Godart, E.; Long, A.; Rosas, R.; Lemercier, G.; Jean, M.; Leclerc, S.; Bouguet-Bonnet, S.; Godfrin, C.; Chapellet, L.-L.; Dutasta, J.-P.; Martinez, A. High-relaxivity Gd(III)–hemicryptophane complex. *Org. Lett.* **2019**, *21*, 1999–2003. (g) Carr, R.; Evans, N. H.; Parker, D. Lanthanide complexes as chiral probes exploiting circularly polarized luminescence. *Chem. Soc. Rev.* **2012**, *41*, 7673–7686. (h) Zhu, Z.; Guo, M.; Li, X.-L.; Tang, J. Molecular magnetism of lanthanide: Advances and perspectives. *Coord. Chem. Rev.* **2019**, *378*, 350–364. (i) Wu, J.; Zhao, L.; Zhang, L.; Li, X.-L.; Guo, M.; Powell, A. K.; Tang, J. Macroscopic

hexagonal tubes of 3 d–4 f metallocycles. *Angew. Chem., Int. Ed.* **2016**, *55*, 15574–15578.

(6) (a) Liu, C. L.; Zhang, R. L.; Lin, C. S.; Zhou, L. P.; Cai, L. X.; Kong, J. T.; Yang, S. Q.; Han, K. L.; Sun, Q. F. Intraligand charge transfer sensitization on self-assembled Europium tetrahedral cage leads to dual-selective luminescent sensing toward anion and cation. *J. Am. Chem. Soc.* **2017**, *139*, 12474–12479. (b) Guo, X.-Q.; Zhou, L.-P.; Cai, L.-X.; Sun, Q.-F. Self-assembled bright luminescent lanthanide-organic polyhedra for ratiometric temperature sensing. *Chem. - Eur. J.* **2018**, *24*, 6936–6940. (c) Yan, L. L.; Tan, C. H.; Zhang, G. L.; Zhou, L. P.; Bunzli, J. C.; Sun, Q. F. Stereocontrolled self-assembly and self-sorting of luminescent europium tetrahedral cages. *J. Am. Chem. Soc.* **2015**, *137*, 8550–8555. (d) Lo, W.-S.; Zhang, J.; Wong, W.-T.; Law, G.-L. Highly luminescent Sm^{III} complexes with intraligand charge-transfer sensitization and the effect of solvent polarity on their luminescent properties. *Inorg. Chem.* **2015**, *54*, 3725–3727. (e) Wu, S.-Y.; Guo, X.-Q.; Zhou, L.-P.; Sun, Q.-F. Fine-tuned visible and near-infrared luminescence on self-assembled lanthanide-organic tetrahedral cages with triazole-based chelates. *Inorg. Chem.* **2019**, *58*, 7091–7098. (f) Hu, S.-J.; Guo, X.-Q.; Zhou, L.-P.; Cai, L.-X.; Sun, Q.-F. Coordination-assembled lanthanide-organic Ln3L3 sandwiches or Ln4L4 tetrahedron: structural transformation and luminescence modulation. *Chin. J. Chem.* **2019**, *37*, 657–662. (g) Li, S.-C.; Cai, L.-X.; Zhou, L.-P.; Guo, F.; Sun, Q.-F. Supramolecular synthesis of coumarin derivatives catalyzed by a coordination-assembled cage in aqueous solution. *Sci. China: Chem.* **2019**, *62*, 713–718. (h) Bing, T. Y.; Kawai, T.; Yuasa, J. Ligand-to-ligand interactions that direct formation of D₂-symmetrical alternating circular helicate. *J. Am. Chem. Soc.* **2018**, *140*, 3683–3689. (i) Yeung, C.-T.; Yim, K.-H.; Wong, H.-Y.; Pal, R.; Lo, W.-S.; Yan, S.-C.; Yee-Man Wong, M.; Yufit, D.; Smiles, D. E.; McCormick, L. J.; Teat, S. J.; Shuh, D. K.; Wong, W.-T.; Law, G.-L. Chiral transcription in self-assembled tetrahedral Eu4L6 chiral cages displaying sizable circularly polarized luminescence. *Nat. Commun.* **2017**, *8*, 1128. (j) Ito, H.; Shinoda, S. Chirality sensing and size recognition of N-Boc-amino acids by cage-type dimeric lanthanide complexes: chirality detection of N-Boc-aspartate anions via luminescence colour change. *Chem. Commun.* **2015**, *51*, 3808–3811. (k) Hamacek, J.; Poggiali, D.; Zebret, S.; Aroussi, B. E.; Schneider, M. W.; Mastalerz, M. Building large supramolecular nanocapsules with europium cations. *Chem. Commun.* **2012**, *48*, 1281–1283. (l) Zhou, Y.; Li, H.; Zhu, T.; Gao, T.; Yan, P. A highly luminescent chiral tetrahedral Eu4L4(L')₄ cage: chirality induction, chirality memory, and circularly polarized luminescence. *J. Am. Chem. Soc.* **2019**, *141*, 19634–19643. (m) Xu, J.; Corneille, T. M.; Moore, E. G.; Law, G.-L.; Butlin, N. G.; Raymond, K. N. Octadentate cages of Tb(III) 2-hydroxyisophthalamides: a new standard for luminescent lanthanide labels. *J. Am. Chem. Soc.* **2011**, *133*, 19900–19910. (n) Alpha, B.; Balzani, V.; Lehn, J.-M.; Perathoner, S.; Sabbatini, N. Luminescence probes: The Eu3⁺ and Tb3⁺-cryptates of polypyridine macrobicyclic ligands. *Angew. Chem., Int. Ed. Engl.* **1987**, *26*, 1266–1267.

(7) (a) Castilla, A. M.; Ousaka, N.; Bilbeisi, R. A.; Valeri, E.; Ronson, T. K.; Nitschke, J. R. High-fidelity stereochemical memory in a FeII4L4 tetrahedral capsule. *J. Am. Chem. Soc.* **2013**, *135*, 17999–18006. (b) Percástegui, E. G.; Mosquera, J.; Ronson, T. K.; Plajer, A. J.; Kieffer, M.; Nitschke, J. R. Waterproof architectures through subcomponent self-assembly. *Chem. Sci.* **2019**, *10*, 2006–2018. (c) Zhang, D.; Ronson, T. K.; Guryel, S.; Thoburn, J. D.; Wales, D. J.; Nitschke, J. R. Temperature controls guest uptake and release from Zn4L4 tetrahedra. *J. Am. Chem. Soc.* **2019**, *141*, 14534–14538.

(8) (a) Wang, W.; Wang, Y.-X.; Yang, H.-B. Supramolecular transformations within discrete coordination-driven supramolecular architectures. *Chem. Soc. Rev.* **2016**, *45*, 2656–2693. (b) Zhang, T.; Zhou, L. P.; Guo, X. Q.; Cai, L. X.; Sun, Q. F. Adaptive self-assembly and induced-fit transformations of anion-binding metal-organic macrocycles. *Nat. Commun.* **2017**, *8*, 15898. (c) Freye, S.; Michel, R.; Stalke, D.; Pawliczek, M.; Frauendorf, H.; Clever, G. H. Template control over dimerization and guest selectivity of interpenetrated coordination cages. *J. Am. Chem. Soc.* **2013**, *135*, 8476–8479.

(d) Riddell, I. A.; Ronson, T. K.; Clegg, J. K.; Wood, C. S.; Bilbeisi, R. A.; Nitschke, J. R. Cation- and anion-exchanges induce multiple distinct rearrangements within metallosupramolecular architectures. *J. Am. Chem. Soc.* **2014**, *136*, 9491–9498.

(9) Li, X. Z.; Zhou, L. P.; Yan, L. L.; Yuan, D. Q.; Lin, C. S.; Sun, Q. F. Evolution of luminescent supramolecular lanthanide M_2nL_3n complexes from helicates and tetrahedra to cubes. *J. Am. Chem. Soc.* **2017**, *139*, 8237–8244.

(10) (a) Li, X. Z.; Zhou, L. P.; Yan, L. L.; Dong, Y. M.; Bai, Z. L.; Sun, X. Q.; Diwu, J.; Wang, S.; Bunzli, J. C.; Sun, Q. F. A supramolecular lanthanide separation approach based on multivalent cooperative enhancement of metal ion selectivity. *Nat. Commun.* **2018**, *9*, 547. (b) Li, X.-Z.; Zhou, L.-P.; Hu, S.-J.; Cai, L.-X.; Guo, X.-Q.; Wang, Z.; Sun, Q.-F. Metal ion adaptive self-assembly of photoactive lanthanide-based supramolecular hosts. *Chem. Commun.* **2020**, *56*, 4416–4419.

(11) (a) Palomo, C.; Oiarbide, M.; Laso, A. Recent advances in the catalytic asymmetric nitroaldol (Henry) reaction. *Eur. J. Org. Chem.* **2007**, *2007*, 2561–2574. (b) Luzzio, F. A. The Henry reaction: recent examples. *Tetrahedron* **2001**, *57*, 915–945.

(12) (a) Shibasaki, M.; Yoshikawa, N. Lanthanide complexes in multifunctional asymmetric catalysis. *Chem. Rev.* **2002**, *102*, 2187–2210. (b) Sasai, H.; Itoh, N.; Suzuki, T.; Shibasaki, M. Catalytic asymmetric nitroaldol reaction: An efficient synthesis of (S) propranolol using the lanthanum binaphthol complex. *Tetrahedron Lett.* **1993**, *34*, 855–858.

(13) Sheldrick, G. M. A short history of SHELX. *Acta Crystallogr., Sect. A: Found. Crystallogr.* **2008**, *64*, 112–122.

(14) Spek, A. L. Single-crystal structure validation with the program. *J. Appl. Crystallogr.* **2003**, *36*, 7–13.